

XAFS investigations of tin nitrides

Dirk Lützenkirchen-Hecht, Nicole Scotti, Herbert Jacobs and Ronald Frahm

Copyright © International Union of Crystallography

Author(s) of this paper may load this reprint on their own web site provided that this cover page is retained. Republication of this article or its storage in electronic databases or the like is not permitted without prior permission in writing from the IUCr.

XAFS investigations of tin nitrides

Dirk Lützenkirchen-Hecht^a, Nicole Scotti^b, Herbert Jacobs^b and Ronald Frahm^a^aInstitut für Materialwissenschaften und FB 8 Physik, Bergische Universität Gesamthochschule Wuppertal, Gaußstr. 20, 42097 Wuppertal, Germany, and^bFachbereich Chemie, Universität Dortmund, Otto-Hahn-Str. 6, 44227 Dortmund, Germany
Email: dirklh@uni-wuppertal.de

Tin nitrides (Sn_3N_4) prepared by the reaction of Sn-halides with KNH_2 in liquid ammonia and a subsequent vacuum annealing procedure were investigated with transmission mode XAFS experiments. While the near edge data suggest the presence of a univalent Sn-compound with a valency close to +4, the analysis of the extended X-ray absorption fine structure proves the presence of two different local Sn sites in this crystal structure: While Sn(1) is surrounded by 4 nitrogen in a distance of 2.06 Å, each Sn(2) ion is coordinated with 6 nitrogen at about 2.17 Å radial distance.

Keywords: XAFS, tin-nitride, Sn_3N_4 , spinell structure.

1. Introduction

Nitrides of the 4th group of the periodic table have attracted much interest since the discovery of the outstanding chemical and physical properties of Si_3N_4 (Lange, Wötting & Winter, 1991). Tin nitrides are of special interest due to their promising semiconducting and electrochromic properties (see Inoue *et al.*, 1998). They can be prepared e.g. by reactive sputtering techniques (Remy & Hantzpergue, 1975, Lima *et al.*, 1991, Maruyama & Morishita, 1995, Inoue *et al.*, 1998) or chemically by the reaction of tin halides (SnBr_2 , SnBr_4 or SnI_4) with potassium amide (KNH_2) and thermal decomposition of the formed intermediate tin imides (Maya, 1991, Scotti *et al.*, 1999). Depending on the details of the preparation procedures, amorphous as well as crystalline structures with varying atomic concentrations of Sn and N have been reported (Remy & Hantzpergue, 1975, Lima *et al.*, 1991, Maruyama & Morishita, 1995, Inoue *et al.*, 1998, Scotti *et al.*, 1999). The XAFS-measurements described here were performed for a detailed investigation of the local atomic arrangement around Sn in chemically prepared tin nitrides with a stoichiometric composition Sn_3N_4 . The results were compared to the distances and coordination numbers derived for the different proposed structures.

2. Experimental details

The chemical synthesis of Sn_3N_4 comprised the reaction of Sn(II)Br_2 with KNH_2 (substance quantity ratio 1:2) in liquid ammonia at 243 K for two days. After the evaporation of excess NH_3 , the solid residue was annealed under vacuum at 573–623 K for 2–5 days (Scotti, 1999). The X-ray diffraction analysis of the resulting dark brown powder revealed diffraction peaks of Sn_3N_4 and contaminations of KBr and metallic Sn (Scotti, 1999, Scotti *et al.*, 1999). In a second series of experiments, SnI_4 was chosen as starting point for the ammonolysis. In this case KI but no metallic Sn was found after the thermal treatment of the intermediate species (Scotti, 1999). Although KBr and KI did not influence the X-ray absorption experiments, their contributions can be significantly reduced by prolonged washing of the samples with water. In addition, metallic

tin can be dissolved in concentrated hot HCl, leading to a pure Sn_3N_4 phase after rinsing with water, centrifugation and drying (Scotti *et al.*, 1999). According to X-ray and neutron diffraction data, the space group of Sn_3N_4 is $\text{Fd}\bar{3}m$ (MgAl_2O_4 -spinnel structure, Wyckhoff, 1968) with $Z=8$ and $a=9.037$ Å (Scotti *et al.*, 1999).

The X-ray experiments were performed at the RÖMO II beamline (Frahm, 1989) at the DORIS III storage ring at HASYLAB (Hamburg, Germany) operating at a positron energy of 4.43 GeV with 75–150 mA of stored current. The data were collected with a double-crystal monochromator using two flat Si(311) and Si(511) crystals. Suppression of higher harmonics was achieved by detuning both monochromator crystals to about 30% of the maximum intensity. Transmission EXAFS data were collected in the vicinity of the Sn K-edges at 29200.1 eV at room temperature and in a liquid nitrogen filled cryostat at about 80 K. We used Ar- and Kr-filled ionization chambers as detectors for the incoming and transmitted intensities. The energy scale of the monochromator was calibrated with a tin metal foil of 25 µm thickness measured in transmission between the second and a third ionization chamber simultaneously with each sample. White tetragonal Sn and crystalline SnO and SnO_2 powders pressed in polyethylene were measured in transmission to obtain reference spectra.

3. Results and Discussion

In Fig. 1, normalized near edge spectra of the chemically synthesized Sn_3N_4 and some Sn reference compounds are presented. Obviously, the absorption edge position shifts towards higher photon energies with increasing Sn valency as can be expected. In the insert of Fig. 1, the absorption edge positions determined as the first inflexion points of the respective absorption spectra are presented as a function of the Sn valency. A commonly applied procedure involves a linear regression between the edge energies of the reference compounds and their valencies and an interpolation of the measured

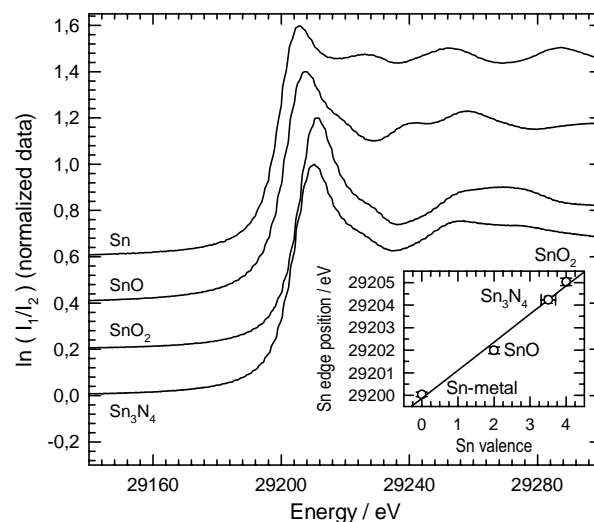


Figure 1:

Near edge X-ray absorption spectra of metallic Sn, SnO, SnO_2 and chemically synthesized Sn_3N_4 in the vicinity of the Sn K-edge (29200.1 eV) measured at room temperature. Insert: Absorption edge position as a function of the Sn valency. A linear interpolation yields a formal value of 3.51 ± 0.20 for the Sn_3N_4 samples.

absorption edge position of the species under investigation to the regression line (see, e.g. Chen *et al.*, 1994, Mansour *et al.*, 1994). In our case, this interpolation leads to a value of about 3.5 ± 0.2 for the oxidation state of the tin ions in chemically prepared Sn_3N_4 . This value agrees qualitatively well with the result of a previous study, where a +4 oxidation state was derived for the Sn ions (Scotti *et al.*, 1999).

In Fig. 2, the magnitudes of the Fourier-Transforms (FT's) of the k^3 -weighted fine structure data obtained from three chemically synthesized Sn_3N_4 samples are presented; the insert depicts a typical raw data set $\chi(k)*k^3$. All data were measured at 80 K. According to the X-ray diffraction data, the N-atoms in the Sn_3N_4 lattice are arranged in a distorted close-packed cubic structure, in which 1/8 of the tetrahedral vacancies are filled with Sn(1)-ions and 1/2 of the octahedral vacancies are filled with Sn(2)-ions, leading to a tetrahedral coordination of Sn(1) with 4 N and a sixfold coordination of Sn(2) (Scotti, 1999). Therefore, the peak doublet at around 1.5 Å radial distance corresponds to the above mentioned Sn(1)-N and Sn(2)-N bonds at 2.05 Å and 2.20 Å, respectively. Furthermore, the peaks between 2.5 Å and 4 Å can be attributed mainly to Sn-Sn interactions at 3.19 Å and 3.74 Å, overlapping however with Sn-N bonds at 3.76 Å, 3.907 Å, 3.811 Å and 3.94 Å. The differences between the shown FT's – clearly visible in the range between ca. 2.5 Å and 3.7 Å radial distance – are probably due to the chemical preparation and purification of the samples. Especially metallic Sn, which has its most prominent contributions in the same distance range, was detected as contaminant by XRD. Different Sn contents may easily cause the observed behaviour.

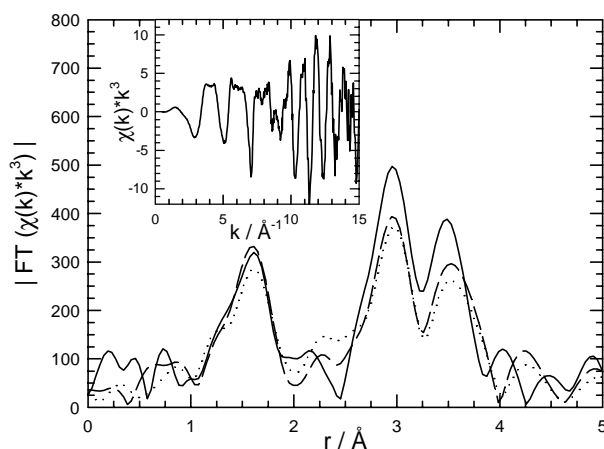


Figure 2:

Fourier-Transforms of the EXAFS spectra ($\chi(k)*k^3$) at the Sn K-edge at 29200 eV of three chemically prepared Sn_3N_4 samples. All measurements were performed at 80 K (k -range for the FT's: 1.88 - 14.6 Å⁻¹, data not phase shift corrected). The insert depicts a measured $\chi(k)*k^3$ raw data set.

For the further data evaluation, the peak between 1 Å and 2 Å was isolated by means of a filter function, back-transformed into k -space and fitted with phases and amplitudes calculated by FEFF (Rehr *et al.*, 1992) using two independent Sn-N coordination shells. A typical fit result is presented in Fig. 3. It has to be mentioned that the beat node at about 12 Å⁻¹ – which results from two coordination shells with slightly different bond distances (Martens *et al.*, 1977) – must be included in the fitted k -range in order to obtain a converging fit. Therefore the upper k limit of the fit should amount to at least ≈ 14 Å⁻¹. Quantitative results of the fit procedure are summarized in Tab. 1; for comparison, the structural data obtained by X-ray diffraction are also presented. In general, the bond distances

determined by the analysis of the XAFS data are slightly smaller than those calculated from the diffraction data. However, the analysis of the X-ray absorption measurements is in reasonable agreement with the results of the X-ray diffraction data evaluation, i.e. Sn(1) ions are surrounded by 4 nitrogen in a distance of about 2.06 Å and each Sn(2) ion is coordinated with 6 nitrogen at ≈ 2.17 Å. It should be mentioned that the fits were also done using only one single Sn-N shell as assumed by the hexagonal structures proposed for tin nitride by other authors (Lima *et al.*, 1991, Maruyama & Morishita, 1995, Inoue *et al.*, 1998); an example of such a fit is also included in Fig. 3. While the determined Sn-N coordination number $N=6.6 \pm 0.5$ agrees qualitatively well with that expected for a hexagonal structure ($N=6$), the resulting bond distance of 2.12 Å is much smaller than the value of $R=2.46$ Å which is expected for hexagonal Sn-nitride. In addition, the quality of the fit is poor for the whole k range and it additionally can not reproduce the beat node so that our results can not give any evidence for the presence of a hexagonal Sn-nitride structure.

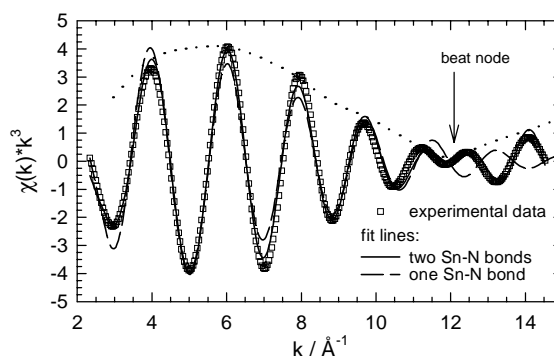


Figure 3:

Typical fit (k range 2.3 Å⁻¹–14.5 Å⁻¹) of the back-transformed Sn-N shell data (radial distance 1 Å < r < 2 Å) with a single (dashed line) and a two shell model (full line). The envelope function of the XAFS oscillations is indicated by a dotted line and reveals a minimum (beat node) for $k_E \approx 12.1$ Å⁻¹.

Table 1:

EXAFS results for the first and second Sn-N coordinations of chemically synthesized Sn_3N_4 . Coordination numbers and radii calculated from the crystallographic structure (Scotti *et al.*, 1999) are given for comparison.

Coordination	XAFS data analysis		Crystallographic data
	R_i / Å		
Sn(1) – N	N_1	4.06 ± 0.10	4
	σ_1 / Å	0.038 ± 0.002	--
	R_2 / Å	2.174 ± 0.001	2.177
Sn(2) – N	N_2	5.70 ± 0.10	6
	σ_2 / Å	0.046 ± 0.002	--

In addition to the conventional XAFS data analysis, an estimate for the difference ΔR of the Sn-N bond distances $\Delta R=R_2-R_1$ can be derived from the beat node by $\Delta R=n\pi/2k_E$, where k_E is the local minimum of the envelope function of the two shells and n is the n^{th} node (Martens *et al.*, 1977). In the present case, $k_E \approx 12.1$ Å⁻¹ represents the first node, which leads to $\Delta R \approx 0.13$ Å, in compared to 0.11 Å and 0.07 Å as determined by XAFS and XRD data analysis respectively.

A more detailed data analysis was also performed for higher coordination shells, namely the peaks located in the FT between ca. 2.5 Å and 3.9 Å (see Fig. 2). Supposed that Sn_3N_4 crystallizes in the above mentioned spinell structure, peaks in the FT in this distance range would correspond to two different Sn-Sn and additional three Sn-N bonds, so that a quantitative analysis of this data set seems to be impracticable due to the complexity of the structure. On the other hand, the Sn-Sn coordinations always have lower bond distances and higher coordination numbers compared to the Sn-N bonds. In addition, due to the monotonically decreasing backscattering amplitude of nitrogen and the resonating behaviour of the Sn backscattering amplitude, the influence of the N backscatterers is further reduced in the k range above ca. 6 \AA^{-1} . We therefore used a two shell model (two Sn-Sn coordinations) and restricted the fit of the back transformed data to the k -range between 6.3 and 14.3 \AA^{-1} . This choice seems to be justified by the fact that the accuracy obtained for all structural parameters is better in such an approximation which involves a two shell model only rather than a five shell fitting procedure. It should be mentioned that a similar procedure has formerly been applied successfully for the investigation of higher order shells in crystalline SnO_2 and SnO_2 hydrogels in the past (Briois *et al.*, 1995). In Fig. 4, a typical fit of the isolated and back-transformed peaks between 2.5 and 3.9 Å is presented. Again, the bond distances determined for the two Sn-Sn coordinations correspond well to the spinell structure determined with X-ray diffraction, i.e. ($R_3=3.225\pm 0.001 \text{ \AA}$ and $R_4=3.742\pm 0.002 \text{ \AA}$ compared to $R_3=3.195 \text{ \AA}$ and $R_4=3.747 \text{ \AA}$, respectively, while the hexagonal structure mentioned above would yield $R=3.69 \text{ \AA}$). In addition, also the determined coordination numbers $N_3=6.6\pm 0.2$, $N_4=11.6\pm 0.6$ can be related to those of the spinell structure ($N_3=6$, $N_4=18$).

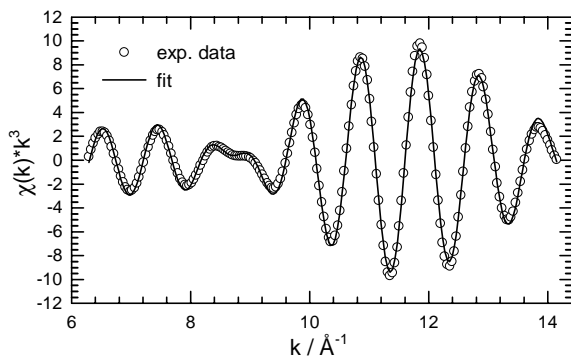


Figure 4:

Typical fit of the back-transformed coordinations between 2.5 Å and 3.9 Å with a two shell model (two individual Sn-Sn coordinations). The fit was performed for $6.3 \text{ \AA}^{-1} \leq k \leq 14.3 \text{ \AA}^{-1}$.

The analysis of the beating node of these back-transformed data did not yield reasonable values for the differences of the two involved Sn-Sn bond distances, i.e. $\Delta R=0.45 \text{ \AA}$ and $\Delta R=0.37 \text{ \AA}$ from the first and second node at 3.5 \AA^{-1} and 8.6 \AA^{-1} , in contrast to 0.52 \AA and 0.55 \AA from the EXAFS and XRD data evaluations, respectively. This discrepancy might be related to the influence of the Sn-backscattering amplitude as well as to the neglected Sn-N bonds, which both can significantly modify the absorption fine structure, especially in the lower k range below ca. 6 \AA^{-1} .

4. Conclusions

XAFS experiments were performed for a detailed investigation of the local structure around Sn in chemically synthesized tin nitride Sn_3N_4 . Near edge X-ray absorption data suggest a tin valence of about 3.50 ± 0.20 , a value which is close to the Sn^{4+} oxidation state which was recently published (Scotti *et al.*, 1999). The evaluation of the extended X-ray absorption fine structure data is conform with the assumption of a spinell structure (MgAl_2O_4 -type) in which two different Sn-sites are present: Sn(1) is coordinated by 4 N in a distance of 2.06 \AA , and Sn(2) is in an octahedral symmetry with 6 N at about 2.17 \AA radial distance. Sn-Sn coordination distances were determined to 3.23 \AA and 3.74 \AA , respectively. The presented data are not at all consistent with hexagonal structures which were proposed for Sn_3N_4 by other groups (Lima *et al.*, 1991, Inoue *et al.*, 1998). Such a hexagonal lattice can neither explain the splitted peaks observed for the Sn-N coordinations at about $2\text{-}2.2 \text{ \AA}$ distance, nor the doublet detected for the Sn-Sn coordinations at $\approx 3.2 \text{ \AA}$ and $\approx 3.75 \text{ \AA}$. Furthermore, this hexagonal crystal structure suggest Sn-N and Sn-Sn bond lengths of 2.46 \AA and 3.69 \AA in contrast to the determined values given above.

Acknowledgement

We like to thank A. Krämer, P. Keil and S. Grundmann for their invaluable help at the beamline. Financial support by HASYLAB and the Ministerium für Schule und Weiterbildung, Wissenschaft und Forschung des Landes Nordrhein-Westfalen is gratefully acknowledged.

References:

- Briois, V.; Santilli, C.V.; Pulcinelli, S.H.; Brito, G.E.S. (1995) *J. Non Cryst. Solids* **191**, 17-28.
- Chen, J.G., Kim, C.M., Frühberger, B., de Vries, B.D. & Touvelle, M.S. (1994) *Surf. Sci.* **321**, 145-155.
- Frahm, R. (1989). *Rev. Sci. Instr.* **60**, 2515 – 2518.
- Inoue, Y., Nomiya, M. & Takai, O. (1998) *Vacuum* **51**, 673-676.
- Lima, R.S., Dionisio, P.H., Schreiner, W.H. & Achete, C. (1991) *Sol. State Commun.* **79**, 395-398.
- Lange, H., Wötting, G. & Winter, G. (1991) *Angew. Chemie* **103**, 1606-1625.
- Mansour, A.N., Melendres, C.A., Pankuch, M. & Brizzolara, R.A. (1994), *J. Electrochem. Soc.* **141**, L69-L71.
- Martens, G., Rabe, P., Schwentner, N. & Werner, A. (1977) *Phys. Rev. Lett.* **39**, 1411-1414.
- Maruyama, T. & Morishita, T. (1995) *J. Appl. Phys.* **77**, 6641-6645.
- Maya, L. (1992) *Inorg. Chem.* **31**, 1958-1960.
- Rehr, J.J., Albers, R.C. & Zabinsky, Z.I. (1992) *Phys. Rev. Lett.* **69** 3397-3400.
- Remy, J.C. & Hantzpergue, J.J. (1975) *Thin Sol. Films* **30**, 197-204.
- Scotti, N. (1999) PhD-Thesis, Universität Dortmund, Germany.
- Scotti, N., Kockelmann, W., Senker, J., Traßel, S. & Jacobs, H. (1999) *Z. Anorg. Allg. Chem.* **625**, 1435-1439.
- Wyckhoff, R.W.G. (1968) *Crystal Structures*, Vol. 4, 2nd ed. New York: Interscience Publishers.